

Radiative Versus Nonradiative Decay Processes in Germanium Nanocrystals Probed by Time-resolved Photoluminescence Spectroscopy

P. K. Giri¹, R. Kesavamoorthy², B. K. Panigrahi², and K.G.M. Nair²

¹Department of Physics, Indian Institute of Technology Guwahati, Guwahati 781039, India

²Materials Science Division, Indira Gandhi Center for Atomic Research, Kalpakkam 603102, India

ABSTRACT

Ge nanocrystals (NCs) of diameter 4–13 nm are grown embedded in a thermally grown SiO₂ layer by Ge ion implantation and subsequent annealing. Steady state and time-resolved photoluminescence (PL) studies are performed on these embedded Ge nanocrystals to understand the origin of the PL emission at room temperature. Steady state PL spectra show a broad peak consisting of a peak at ~2.1 eV originating from Ge NCs and another peak at ~2.3 eV arising from ion-beam induced defects in the Ge/SiO₂ interface. Time-resolved PL studies reveal double exponential decay dynamics of the PL emission on the nanoseconds time scale. The faster component of the decay with large amplitude and having a time constant $\tau_1 \sim 3.1$ ns is attributed to the nonradiative lifetime, since the time constant reduces with increasing defect density. The slower component with time constant $\tau_2 \sim 10$ ns is attributed to radiative recombination at the Ge NCs. These results are in close agreement with the theoretically predicted radiative lifetime for small Ge NCs.

INTRODUCTION

Over the last decade, studies on the optical properties of group IV semiconductor nanocrystals (NCs) have attracted much interest because of their potential applications in Si-based optoelectronics, nanophotonics, and electronic/optical memory devices. Si NCs of several nanometers in diameter show indirect band gap nature [1] and this results in a relatively long photoluminescence (PL) lifetime [2], which is one of the main obstacles to realizing Si-based light emitting devices. In contrast, Ge NCs show a stronger confinement effect [3] resulting in a direct gap semiconductor nature [4]. There have been several theoretical predictions on the superior optical properties of Ge NCs [5] as compared to the Si NCs. However, there is a lack of consensus about the origin of intense visible PL from Ge NCs [6,7]. While majority of the reports have indicted that the defects in the host matrix are primarily responsible for broad PL in the visible region [8,9], some studies have attributed the visible and near-infrared PL to the Ge NCs. Size dependent near-infrared PL [10] and fast ($\ll 1$ μ s) PL decay dynamics [11] from Ge NCs have been attributed to quantum confinement effects, though later studies showed that the deep traps in the gap states of NC Ge are responsible for such emission [9,12].

A powerful technique to explore dynamical characteristics of the carriers that contribute to the PL is time-resolved PL spectroscopy. While theoretical studies predict several orders of magnitude lower lifetime in NC Ge (typically a few ns) as compared to NC Si (typically in the range μ s–ms) [13,14], there is a lack of experimental evidence in support of the prediction. Hence, experimental determination of the radiative lifetime in NC Ge is essential to explore fully its potential applications.

In this work, we study the steady state and transient decay characteristics of the photoluminescence from embedded Ge NCs with varying size and surrounding defect density. From the steady state PL measurements, we first isolate the origin of various PL bands. Relative contribution of radiative and nonradiative recombination in Ge NCs is evaluated from time-resolved studies. Our results are compared with the theoretically predicted radiative lifetime of Ge NCs.

EXPERIMENTAL DETAILS

CZ grown Si (100) wafers are used as the substrates for growing SiO₂ layers of thickness ~300 nm by wet oxidation method. Ge NCs are synthesized by implanting 300 keV Ge⁺ ions at room temperature on the SiO₂ layer with doses 3×10^{16} (Ge1), 1×10^{17} (Ge2) and 2×10^{17} (Ge3) ions/cm². Implanted samples were heat-treated at 800°C for 1 hour and further treated at 950°C for 2 hours in inert gas ambient. Glancing incidence X-ray diffraction (XRD) and Raman scattering measurements were used to detect the formation of Ge NCs in SiO₂ after each step of annealing. Steady state PL measurements were performed at room temperature with 488 nm laser excitation. The PL decay measurements were performed at RT using 495 nm excitation pulse of 1.32 ns duration using a commercial fluorescence lifetime setup with a time resolution of 0.113 ns. In the decay measurement, a cutoff filter was placed before the emission detector to block the light below the wavelength 550 nm.

RESULTS AND DISCUSSION

Figure 1 shows a set of XRD spectra on annealed Ge2 and Ge3 samples. Curve 1 in Figure 1 is for Ge2 sample annealed at 800°C, curves 2 and 3 are for Ge2 sample annealed at 950°C with different grazing angle of incidence, and curve 4 is for Ge3 post annealed at 950°C. Strong Bragg peak at 26.44° and a weak peak at ~27.4° (shown with arrow) in curve 1 correspond to GeO₂ and Ge (111) NCs, respectively [5]. Due to the very small size of the NCs grown after annealing at 800°C, Ge related peak in XRD spectra is very weak. After 950°C annealing, Ge(111) peak became distinct due to larger size of the NCs as shown in curves 2 and 4. Curve 3 shows Ge (311) peak obtained with different angle (3°) of grazing incidence on Ge2 sample annealed at 950°C. To determine the size of the NCs, we recorded low frequency Raman scattering (LFRS) spectra (not shown) on these samples. LFRS spectra of 800°C annealed samples show a peak at 21.2 cm⁻¹ in Ge1 and 15.7 cm⁻¹ in Ge2 sample. After 950°C annealing, these peaks shift to 13.8 cm⁻¹ and 6.5 cm⁻¹, respectively, indicating an increase in the NC size. The average diameter of the NCs as estimated from LFRS spectra varies from 4 to 13 nm depending on the ion dose and annealing temperature. Detailed of these results will be treated elsewhere [15]. Our studies show that nanocrystallite size is smaller in highest dose sample as compared to the intermediate dose sample. This may be partly related to the highly damaged lattice with high dose implantation that hinders the growth of the NCs. Another possible reason could be the implantation at high dose rate caused a black coating on the sample surface that might have caused the SiO₂ layer to receive a lesser dose than the expected dose (2×10^{17} ions/cm²). Thus smaller size nanocrystallites in highest dose sample may be justified.

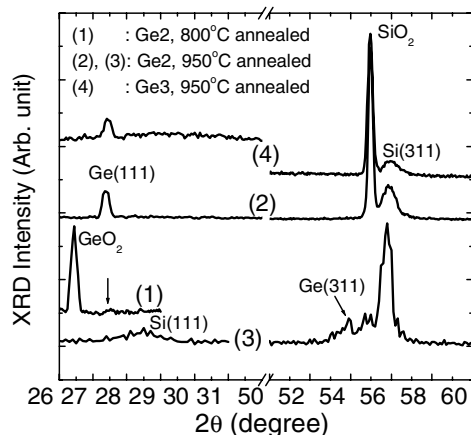


Figure 1. XRD spectra of Ge NCs formed by post-implant annealing at 800°C for Ge2 (curve 1), and 950°C (curve 2, 3 for Ge2, 4 for Ge3). Curve 2 and 3 are obtained for the same Ge2 sample under different grazing angle of incidence.

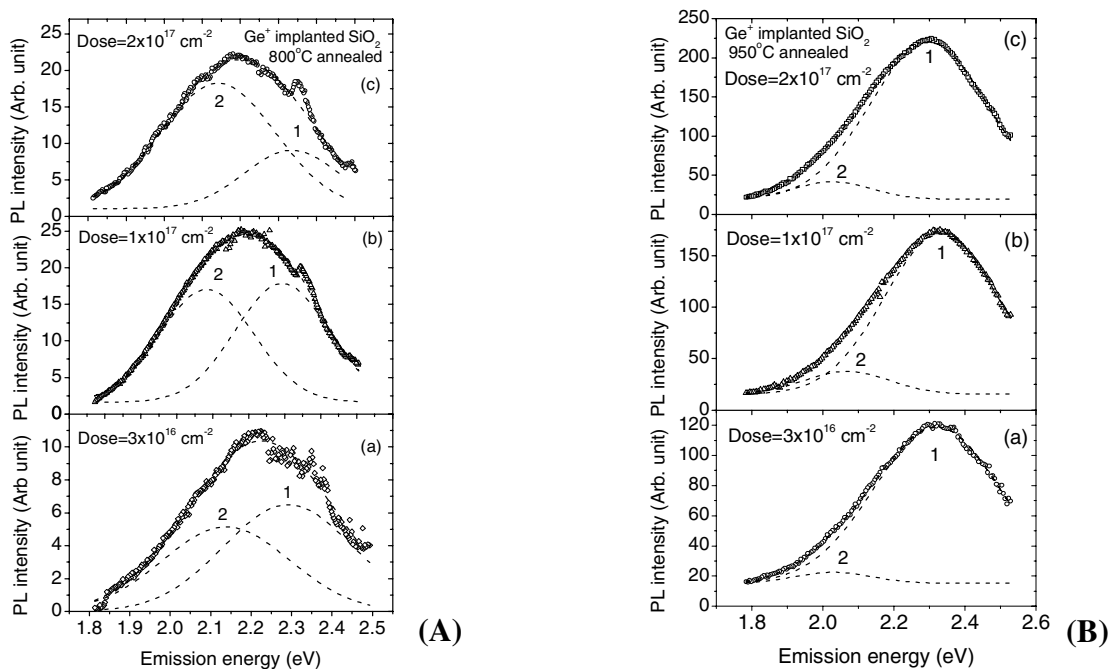


Figure 2. (A) Room temperature PL spectra (with symbols) of NC Ge prepared at 800°C for three different doses: (a) $3 \times 10^{16} \text{ cm}^{-2}$, (b) $1 \times 10^{17} \text{ cm}^{-2}$, (c) $2 \times 10^{17} \text{ cm}^{-2}$. Two Gaussian peaks are fitted (dashed lines) with the experimentally observed PL spectra. Fitting parameters are presented in Table I. (B) PL spectra of same set of samples further annealed at 950°C.

Figure 2(A) and 2(B) shows a set of PL spectra for 800°C and 950°C annealed samples, respectively. The unconvoluted PL spectra of 800°C annealed samples show an intense and broad PL band at $\sim 2.19 \text{ eV}$ for three different doses. After 950°C annealing, the PL peak shifts to $\sim 2.32 \text{ eV}$ as shown in Figure 2(b). This apparent blue-shift of the PL band with increasing annealing temperature is inconsistent with the quantum confinement model of excitonic

recombination in the NCs, since annealing induced increase in size of the NCs (Table I) is expected to show a red-shift of PL peak. Hence, the major contribution to PL emission is unlikely to originate from Ge NCs. A closer look at the asymmetric line shape of the spectra in Figure 2(A) and Figure 2(B) reveals that the observed peak can be resolved into two Gaussian peaks. Fitting parameters thus obtained are shown in Table I. The fitted data show that besides the major peak at ~ 2.3 eV (Peak 1) that is common to all samples, 800°C annealed sample shows a lower energy peak (Peak 2) at ~ 2.1 eV, and after 950°C annealing this peak red-shifts to ~ 2.0 eV, as expected from quantum confinement model. PL peak positions are almost independent of the ion dose, whereas relative peak intensity changes with dose. 800°C annealed samples show comparable intensities for Peak 1 and Peak 2 (see Figure 2) while 950°C annealed samples show that Peak 1 is about 10 times more intense than Peak 2.

Reported results have shown that visible PL from Ge implanted SiO₂ layers primarily arise from a luminescent defect center [12]. In our case, the unimplanted 800°C annealed SiO₂ layers show a weak PL at 2.25 eV that is subtracted as background spectra from the spectra plotted in Figure 2. Table I shows that PL peak at ~ 2.3 eV does not shift with ion dose and annealing conditions.

Table I: Fitting parameters i.e. peak center E and the peak width (FWHM) ΔE of the Gaussian peaks (Peak 1 and peak 2 shown in Figure 2(a) and Figure 2(b)) fitted with the PL spectra observed for different samples. Mean size (diameter, d) of the NCs are determined from the LFRS spectral peak position.

Ge dose (cm ⁻²)	800°C annealing					950°C annealing				
	Peak 1		Peak 2		d (nm)	Peak 1		Peak 2		d (nm)
	E (eV)	ΔE (eV)	E (eV)	ΔE (eV)		E (eV)	ΔE (eV)	E (eV)	ΔE (eV)	
3×10^{16}	2.29	0.32	2.14	0.31	4.0	2.32	0.35	2.03	0.21	6.1
1×10^{17}	2.29	0.26	2.08	0.26	5.4	2.33	0.32	2.06	0.23	13.0
2×10^{17}	2.33	0.25	2.14	0.30	4.1	2.30	0.33	2.03	0.22	9.2

The intensity of this component increases with dose as seen in Figure 2. The defect density increases with dose and the PL intensity is expected to increase with dose from these defects. Hence, the 2.3 eV peak is attributed to defects. 2.3 eV PL peak has been observed by several groups and attributed to defects [8,9] in the host matrix. In the present study, these defects are created by Ge⁺-ion bombardment into SiO₂ and their density changes with dose and post-annealing temperature. Ion beam induced dangling bonds at the NC Ge/SiO₂ interface has been identified as one major defect in such embedded system. Hence, the PL emission from these NCs is dominated by defects at the NC/SiO₂ interface and/or the surrounding SiO₂ matrix. Data presented in Table I show that Peak 2 is red-shifted by about 0.1 eV with the increase of the nanocrystal size from, say, 4.0 nm to 6.1 nm. This is fully consistent with the quantum confinement model of carrier recombination in NCs. Similar observations were made by Kim et al [16] and Maeda et al [6]. Hence, we attribute peak 2 at ~ 2.1 eV to the excitonic recombination at the NC Ge [8].

Figure 3(a) shows the PL decay characteristics of samples implanted with different doses. As 2.3 eV PL band arises from the defects in the embedding matrix, to reduce the defect contribution to experimental decay data we use a 550 nm cutoff filter at the emission end. Reference data shown in Figure 3(a) refers to the system response for the lifetime measurement, which was subtracted from sample data to extract the decay time constant (τ). The experimental data could be fitted well with two exponential decay functions with time constants τ_1 and τ_2 for the entire range of ion doses. Fitting parameters thus obtained (see Figure 3(b)) show that τ_1 decreases from 3.1 ns to 2.5 ns with the increase of dose, while τ_2 does not change appreciably

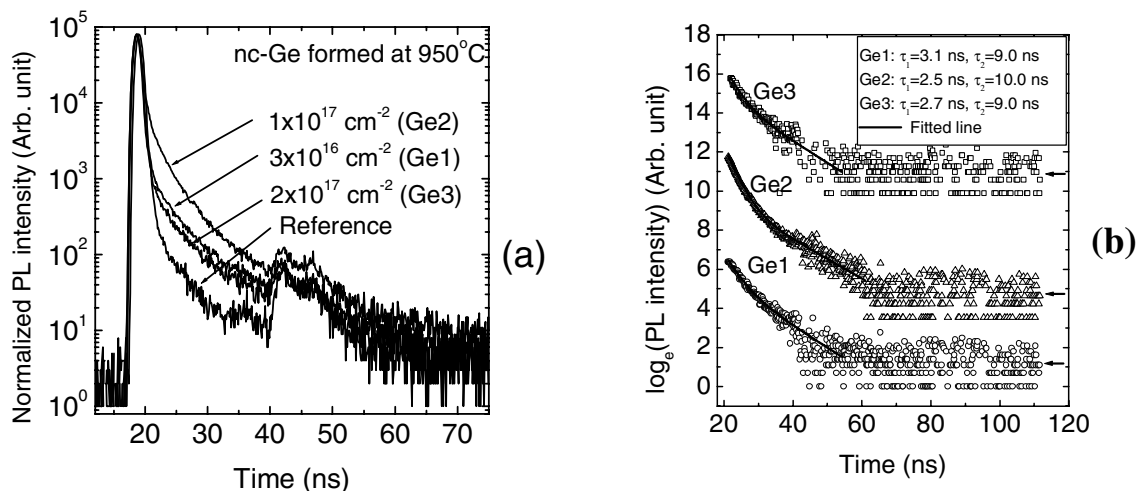


Figure 3. (a) Room temperature PL decay characteristics (symbols) of the Ge NCs (nc-Ge) for samples Ge1, Ge2 and Ge3 annealed at 950°C. System response is shown as ‘reference’ data. (b) Decay characteristics shown after subtracting the reference data from the sample spectra. The experimental data (symbols) are fitted with two exponential decay functions with time constants τ_1 and τ_2 and shown as solid line.

with dose. More interestingly, the ratio of the amplitudes for the fast component and the slow component ranges from 233 to 6142 depending upon the dose. This dose dependence of the τ_1 can be understood by considering the nonradiative recombination at the deep level defects. As the defect density increases with increasing ion dose, nonradiative recombination lifetime is expected to decrease with dose according to the Shockley-Read-Hall recombination theory [17]. Hence, the fast decay component can be attributed to the nonradiative recombination lifetime. In contrast, time constant τ_2 does not change with dose and seems to be a characteristic of the carrier recombination at the Ge NCs. This is consistent with the observation of a low intensity PL band at ~ 2.1 eV from steady state measurement. Note that in contrast to a very large PL lifetime (ranging from μ s to ms) reported for NC Si, NC Ge shows extremely fast (~ 10 ns) decay dynamics.

Theoretically predicted lifetime varies typically from ~ 10 ns [14] to ~ 100 μ s [12] for small NC Ge. As the direct band gap of Ge is very close to the indirect gap of Ge crystals, the PL lifetime for band to band transition in Ge is expected to be quite small as compared to that of Si. Hence, observed fast decay dynamics may be justified. Our results are in close agreement with

the theoretically predicted radiative lifetime of ~ 10 ns for NC Ge [14]. Hence, the observed τ_2 (~ 9 – 10 ns) is a characteristic of the NC Ge, while τ_1 (2.5 – 3.1 ns) is the nonradiative recombination time associated with the defects. The nonradiative relaxation procedure might take place at surface dangling bonds of NC Ge or at the interface between NC Ge and SiO₂ matrix.

CONCLUSIONS

We provide experimental evidence of a fast radiative recombination in Ge NCs. From the steady state PL measurements, we show that the ~ 2.3 eV PL emission from ion-beam synthesized NCs is primarily contributed by the defects in the SiO₂ matrix or at the Ge/SiO₂ interface, whereas the ~ 2.1 eV PL band is attributed to radiative recombination at the Ge NCs. Time-resolved measurements reveal that the fast component ($\tau=2.5$ – 3.0 ns) of the decay is the nonradiative lifetime of carriers, while the slower component ($\tau=9$ – 10 ns) is attributed to the radiative recombination lifetime of carriers at the Ge NCs.

REFERENCES

1. D. Kovalev, H. Heckler, M. Ben-Chorin, G. Polisski, M. Schwartzkopff, F. Koch, *Phys. Rev. Lett.* **81**, 2803 (1998).
2. C. Garcia, B. Garrido, P. Pellegrino, R. Ferre, J.A. Moreno, J. R. Morante, L. Pavesi, M. Cazzanelli, *Appl. Phys. Lett.* **82**, 1595 (2003).
3. C. Bostedt and T. van Burren, T. M. Willey, N. Franco, L. J. Terminello, C. Heske, T. Moller, *Appl. Phys. Lett.* **84**, 4056 (2004).
4. J. R. Heath, J. J. Shiang, A. P. Alivisatos, *J. Chem. Phys.* **101**, 1607 (1994).
5. H.-Ch. Weissker, J. Furthmüller, F. Bechstedt, *Phys. Rev. B* **65**, 155327 (2002); *ibid.*, *Phys. Rev. B* **65**, 155328 (2002).
6. Y. Maeda, *Phys. Rev. B* **51**, 1658 (1995).
7. J. Zhang, X. Bao, Y. Ye, X. Tan, *Appl. Phys. Lett.* **73**, 1790 (1998).
8. K. S. Min, K. V. Shcheglov, C. M. Yang, H. A. Atwater, M. L. Brongersma, A. Polman, *Appl. Phys. Lett.* **68**, (1996) 2511.
9. X. L. Wu, T. Gao, G. G. Siu, S. Tong, X. M. Bao, *Appl. Phys. Lett.* **74**, (1999) 2420.
10. S. Takeoka, M. Fujii, S. Hayashi, K. Yamamoto, *Phys. Rev. B* **58**, 7921 (1998).
11. S. Takeoka, M. Fujii, S. Hayashi, K. Yamamoto, *Appl. Phys. Lett.* **74**, 1558 (1999).
12. Y. M. Niquet, G. Allan, C. Dellerue, M. Lanoo, *Appl. Phys. Lett.* **77**, 1182 (2000).
13. M. Dovrat, Y. Goshen, J. Jedrzejewski, I. Balberg, A. Sa'ar, *Phys. Rev. B* **69**, 155311 (2004).
14. H. -Ch. Weissker, J. Furthmuller, F. Bechstedt, *Phys. Rev. B* **69**, 115310 (2004); *ibid.*, *Phys. Rev. B* **67**, 245304 (2003).
15. P. K. Giri, R. Kesavamoorthy, B. K. Panigrahi, K. G. M. Nair, (Unpublished).
16. H. B. Kim, K. H. Chae, C. N. Whang, J. Y. Jeong, M. S. Oh, S. Im, J. H. Song, *J. Lumin.* **80**, 281 (1999).
17. Jasprit Singh, *Optoelectronics: An introduction to materials and devices*, McGraw-Hill, 1996, Chap 5.